

O.A. BURYI[✉]
S.B. UBISZKII
S.S. MELNYK
A.O. MATKOVSKII

The Q-switched Nd : YAG and Yb : YAG microchip lasers optimization and comparative analysis

Institute of Telecommunications, Radioelectronics and Electronic Engineering,
Lviv Polytechnic National University, Bandery St., 12, Lviv, 79046, Ukraine

Received: 26 August 2003/Revised version: 20 October 2003
Published online: 15 January 2004 • © Springer-Verlag 2004

ABSTRACT The microchip lasers based on the neodymium or the ytterbium doped yttrium-aluminium garnet crystal and Q-switched by the Cr^{4+} : YAG film are considered. The optimal (maximizing of energy) values of the pumping beam radius, the absorber parameters (the thickness and tetravalent chromium ion concentration), and the output mirror reflectivity are determined. The possibility of higher values of energy in the Yb : YAG laser pulse, in comparison with a more traditional Nd : YAG laser, is also substantiated.

PACS 42.60.Gd

1 Introduction

Q-switched microchip lasers are widely investigated and used as compact, relatively high-power coherent radiation sources for the needs of ranging, sensing, and material treatment. Such a laser consists of the generating (usually Nd : YAG) crystal with the Cr^{4+} : YAG saturable absorber layer and the input and output mirrors formed on the cavity edges. The ability to attain saturable absorption near $1 \mu\text{m}$ is provided by the ${}^3A_2 \rightarrow {}^3T_2$ and ${}^3T_2 \rightarrow {}^3T_1$ transitions of the tetrahedrally coordinated tetravalent chromium ions, referred hereinafter as phototropic centers. The quantum efficiency of the Cr^{4+} : YAG absorber is low – the relative losses are about 89% [1].

We consider the problem of the Q-switched microchip laser parameters optimization. It consists of determining the output mirror reflectivity R_2 , the absorber thickness l_s , the tetravalent chromium ion concentration n_{s0} (or the initial transmission $T_0 = \exp(-\sigma_1 n_{s0} l_s)$, where σ_1 is the effective cross-section of the ${}^3A_2 \rightarrow {}^3T_2$ transition), and the pumping beam radius r_p , in order to maximize the energy in the laser pulse (hereinafter simply referred to as energy). The approach to the optimization problem is based on solving the rate equations system [1]. This describes the dynamics of the inversion accumulation in the generating medium, the absorption in Cr^{4+} : YAG film, and photon generation. After that, we compare the results obtained from numerically solving the

rate equations system, with results obtained by use of rough analytical expressions.

Such a comparison enables estimation of the precision of the rough method to be made. In addition, a more rigorous optimization of the modulator thickness l_s and active dopant concentration n_{s0} can be carried out, not only the initial transmission T_0 optimization, as it takes place using analytical expressions.

This optimization allows estimation of the theoretical maximum obtainable value of the energy (as well as the peak power) for different generating media and, consequently, to carry out a comparative analysis. This approach is used here for the comparison of the efficiencies of the microchip lasers based on Nd : YAG and Yb : YAG generating media. This investigation is motivated by certain properties of the Yb^{3+} doped generating medium, which provide the expectation of achieving higher values of pulse energy for a Yb : YAG based microchip laser in comparison with a more traditional Nd : YAG laser.

The advantages of the Yb : YAG medium in comparison with Nd : YAG are: higher pumping efficiency, lower Stox losses (9% for Yb : YAG and 26% for Nd : YAG), low thermal load, a wider absorption band in the pumping region, a higher lifetime of the upper laser level, an absence of concentration quenching, and consequently, the possibility of an ytterbium concentration increase [2, 3].

At the same time, the laser transition cross-section σ_a of an Yb : YAG medium is lower than that of a Nd : YAG laser. As this report will show, the previously mentioned advantages of Yb^{3+} ions cause an appreciable increase in efficiency of the Yb : YAG laser if the optimal pumping beam radius or a sufficiently high pumping power are provided.

2 The microchip Q-switched laser parameters optimization

The method used for the microchip Q-switched laser parameters optimization (output mirror reflectivity R_2 , absorber width l_s , tetravalent chromium ion concentration n_{s0} , pumping beam radius r_p , generating medium length l_a), based on both the rough analytical and numerical analysis of the Xiao–Bass model [1, 4], are represented by a system of differential rate equations. These describe the dynamics of the inversion in the generating medium n_a , the Cr^{4+} ion concentration on the ground level n_s , and the changing photon

✉ Fax: +380-322/742-164, E-mail: crystal@polynet.lviv.ua

quantity q , and are as follows :

$$\begin{cases} \frac{dn_a}{dt} = -n_a \frac{\sigma_a c_0}{V'} q - \frac{n_a}{\tau_{fa}} + W_p (n_{a0} - n_a), \\ \frac{dn_s}{dt} = -n_s \frac{\sigma_1 c_0}{V'} q + \frac{n_{s0} - n_s}{\tau_{fs}}, \\ \frac{dq}{dt} = (2n_a \sigma_a l_a - 2n_s \sigma_1 l_s - 2(n_{i0} - n_s) \sigma_2 l_s - L) \frac{q}{t_r} \\ \quad + \varepsilon \cdot (n_a + n_{a0}) c_0 \sigma_a \frac{l_a}{V'}. \end{cases} \quad (1)$$

Here $c_0 = 3 \times 10^8$ m/s, and n_{a0} is the activator concentration. For Yb [5], $n_{a0} \approx 26.6 \times 10^{20} \text{ cm}^{-3}$, and for Nd [4], $n_{a0} \approx 1.387 \times 10^{20} \text{ cm}^{-3}$.

n_{s0} is the Cr^{4+} concentration, with $n_{s0} \sim 10^{17} \div 10^{19} \text{ cm}^{-3}$ in this case.

σ_a is a cross-section of the laser transition, for Yb : YAG, $\sigma_a = 2 \times 10^{-20} \text{ cm}^2$, and for Nd : YAG, $\sigma_a = 3.5 \times 10^{-19} \text{ cm}^2$.

σ_1 , and σ_2 , are cross-sections of the transitions between absorber levels, here $\sigma_1 = 1.5 \times 10^{-18} \text{ cm}^2$, $\sigma_2 = 1.0 \times 10^{-19} \text{ cm}^2$ (it must be mentioned that different researchers give rather different cross-sectional values for Cr^{4+} : YAG in particular. In [4] it is taken as $2.5 \times 10^{-18} \text{ cm}^2$ for the ${}^3A_2 \rightarrow {}^3T_2$ transition, and as $3.0 \times 10^{-19} \text{ cm}^2$ for the ${}^3T_2 \rightarrow {}^3T_1$ transition).

τ_{fa} is the upper laser level lifetime, for Yb : YAG, $\tau_{fa} = 0.951$ ms, and 0.23 ms for Nd : YAG.

τ_{fs} is the lifetime of the Cr^{4+} excited 3T_2 level, here $\tau_{fs} = 3.5$ μs .

l_a is the generating medium length, here $l_a \sim 1$ mm.

l_s is the absorber thickness, here $l_s \sim 10 \div 250$ μm .

$l' = n(l_a + l_s)$ is the resonator length.

n is the refractive index, here $n = 1.823$ for Yb : YAG, and 1.816 for Nd : YAG.

$t_r = 2l'/c_0$ is the time of the double passing of the resonator.

$W_p = \frac{\eta P_p}{n_g V h \nu_p}$ is the pumping rate.

ηP_p is the effective pumping power.

P_p is the pumping power.

η is the pumping efficiency.

$V = l_a \cdot S$, $S = \pi r_p^2$, where r_p is the pumping beam radius.

n_g is the activator ion concentration on the ground level.

$n_g \approx n_{a0} - n_a$, ν_p is the pumping radiation frequency.

$\nu_p = c_0/\lambda_p$, where λ_p is the pumping radiation wavelength (940 nm for Yb : YAG, and 809 for Nd : YAG).

ε is a dimensionless coefficient characterising the comparative power of the spontaneous radiation, $\varepsilon \approx 10^{-13}$ [6] (the second term of the last equation is in the form offered in [6]).

V' is the effective mode volume, $V' = (l'/l_a)V_a$, where V_a is the mode volume (here we assume $V_a \approx V$).

$L = -\ln R_1 R_2 + L_i$ represents the total loss.

L_i represents diffraction and absorption losses (with the exception of the losses on the transitions ${}^3A_2 \rightarrow {}^3T_2$ and ${}^3T_2 \rightarrow {}^3T_1$ in the absorber), where $L_i \approx 0.03$, and R_1 , R_2 are the input ($R_1 \approx 1$) and output mirrors' reflectivities of the laser radiation wavelength (1030 nm for Yb : YAG and 1064 nm for Nd : YAG).

The quantity of photons in the resonator q in relation to the output power is given by the expression $P(t) = \frac{h\nu}{t_r} \ln\left(\frac{1}{R_2}\right)q(t)$, where ν is the laser radiation frequency. The energy can now

be calculated as $E = \int P(t) dt$, where the integral limits are determined by the pulse duration. All calculations in this chapter are carried out for the Nd : YAG generating medium. The results presented later for Yb : YAG are easily obtained by a corresponding substitution of the generating medium parameters into the equations.

We consider both the numerical method obtained by the fourth order Runge–Kutta technique, and the rough analytical solution of (1). Use of the numerical method allows separate accomplishment of the optimization of the absorber width l_s , and the tetravalent chromium ion concentration n_{s0} , that can otherwise not be realized by the analytical solution. Moreover, this approach allows estimation of the precision of the analytical solution.

The rough analytical solution of (1) may be obtained if the terms described for the pumping and the spontaneous transitions are neglected [4]. In particular, for the peak power and the energy one can obtain:

$$P_{\max} = \frac{h\nu S l'}{t_r} \ln \frac{1}{R_1 R_2} \times \left\{ n_{ai} - n_{af} - \frac{n_{s0} l_s}{l_a} \left(1 - \frac{\sigma_2}{\sigma_1}\right) \left(1 - \left(\frac{n_{af}}{n_{ai}}\right)^{\sigma_1/\sigma_a}\right) - \frac{L_i - \ln(R_1 R_2) + 2\sigma_2 l_s n_{s0}}{2\sigma_a l_a} \ln\left(\frac{n_{ai}}{n_{af}}\right) \right\}, \quad (2)$$

$$E = \frac{h\nu S}{2\sigma_a} \ln(R_1 R_2) \ln\left(\frac{n_{af}}{n_{ai}}\right), \quad (3)$$

where n_{ai} and n_{af} are the inversions in the generating medium before and after the laser pulse irradiation respectively. There is a connection between n_{ai} and n_{af} determined by:

$$n_{ai} - n_{af} - n_{s0} \frac{l_s}{l_a} \left(1 - \frac{\sigma_2}{\sigma_1}\right) \left(1 - \left(\frac{n_{af}}{n_{ai}}\right)^{\sigma_1/\sigma_a}\right) - \frac{L_i - \ln(R_1 R_2) + 2\sigma_2 l_s n_{s0}}{2\sigma_a l_a} \ln\left(\frac{n_{ai}}{n_{af}}\right) = 0. \quad (4)$$

The absorber thickness l_s and the phototropic ion concentration n_{s0} are contained in (4) as a product, so the energy will be a function of the initial transmission $T_0 = \exp(-\sigma_1 l_s n_{s0})$ only (not a function of l_s and n_{s0} separately).

In principle, the optimization problem may be solved by analytical or numerical calculation of the energy E at the values of R_2 , l_s , n_{s0} , r_p , l_a , keeping within their range of definition. However, this problem may be simplified sufficiently if some relation between the values can be established.

2.1 Optimization of the output mirror reflectivity and the absorber initial transmission

The laser pulse generation is started when the amplification in the generating medium becomes equal to the losses, i.e. when the inversion n_a achieves a high enough value of the generation condition to fulfill:

$$2\sigma_a l_a n_a - 2\sigma_1 l_s n_{s0} - L_i + \ln(R_1 R_2) = 0. \quad (5)$$

The 3T_1 absorber level is practically empty before the generation starts, so the term with σ_2 is absent in (5).

The energy goes up if the inversion before the pulse generation n_{ai} increases (at fixed n_{af}). As follows from (5), the inversion n_{ai} is directly proportional to the absorber optical density $D_0 = -\ln T_0 = \sigma_1 l_s n_{s0}$, consequently, the energy rises if the absorber initial transmission decreases. However, the essential decreasing of the initial transmission may lead to the situation that the generation condition (5) is not satisfied at the fixed pumping rate W_p , and the output mirror reflectivity R_2 . This disappearing of the generation is related to the fact that at the fixed pumping rate W_p , the maximal achievable value of the inversion of the laser pulse amounts to $n_{amax} = \frac{\eta P_p}{V h \nu_p} \tau_{fa}$, which follows from the first equation of the system (1), with $q \approx 0$. So, if the initial transmission decreases, the generation disappears when the condition

$$2\sigma_a l_a n_{amax} \geq 2\sigma_1 l_s n_{s0} + L_i - \ln(R_1 R_2) \quad (6)$$

becomes unfeasible, i.e. when the maximal achievable level of the amplification remains less than the losses.

Thus, the decreasing of the initial transmission leads to a rising of the energy until the condition (6) becomes invalid. Obviously, the maximal value of the energy will be achieved at equality in (6), i.e. the nonlinear losses in the absorber will ensure the achievement of the maximal inversion value n_{amax} (more precisely, the left part of (6) must be higher than the right one for a small value). This consideration is illustrated by Fig. 1a, where the results of the calculations of the energy as a function of the initial transmission T_0 and the output mirror reflectivity R_2 are presented. The calculations are carried out with the analytical expressions (3) and (4) using the values: effective pumping power $\eta \cdot P_p = 0.5$ W, generating medium length $l_a = 1$ mm, and pumping beam radius $r_p = 75$ μm . It is obvious from Fig. 1a that the region of the T_0 and R_2 values is subdivided into two subregions, one of them corresponds to the presence of the generation and the another to its absence. The maximal values of the energy are realized on the boundary between these regions, defined, as follows from (6), by:

$$T_0 = \frac{1}{\sqrt{R_1 R_2}} \exp(-\sigma_a l_a n_{amax} + L_i/2). \quad (7)$$

This equation establishes a connection between the optimal values of the initial transmission and the output mirror reflectivity. As can be seen from (7), as $R_1 \rightarrow 0$ the value $T_0 \rightarrow \infty$. Naturally, the withdrawal of T_0 from the range $0 \rightarrow 1$ means

that generation is absent at this value of output mirror reflectivity and any initial transmission value.

Thus, the microchip laser optimization of the initial transmission and the output mirror reflectivity (when the other parameters are fixed) consists of the calculation of the energy along the boundary of the generation region.

As was mentioned above, the analytical expressions contain the absorber thickness l_s , and the phototropic centers concentration n_{s0} , only as a product $l_s \cdot n_{s0}$, so the optimization may be realized on the initial transmission $T_0 = \exp(-\sigma_1 n_{s0} l_s)$. On the other hand, some terms of the system (1) contain the values n_{s0} and l_s (the last one by means of V' and t_r) separately.

The separate optimization of the absorber thickness and the phototropic centers concentration may only be realized numerically. The results of such optimization are presented in Fig. 1b. The three different dependencies correspond to the same value of T_0 connected with R_2 by (7), but to three different values of the concentration n_{s0} , and three different values of the absorber thickness $l_s = \frac{-\ln T_0}{\sigma_1 n_{s0}}$, respectively. As can be seen from Fig. 1b, the phototropic concentration n_{s0} increase at the fixed initial transmission leads to a definite increase of the energy.

The maximal achievable values of the energy at other parameters mentioned above amounted to 51.7, 53.1, and 58.5 μJ , for the concentrations $n_{s0} = 10^{17}$, 10^{18} , and 10^{19} cm^{-3} , respectively (the last of these values is approximately equal to the highest technologically reachable concentration [7]). Relative energy increases amounts to $\sim 13\%$ of the concentration increases from 10^{17} cm^{-3} to 10^{19} cm^{-3} . As can be seen from Fig. 1a, the analytical calculation gives the value of 51.9 μJ for the maximal achievable energy, which corresponds to an inaccuracy of $\sim 12.7\%$ if the phototropic centers concentration is close to the maximal technologically reachable. Thus, the tetravalent chromium ion concentration increases with a synchronous decreasing of the absorber thickness (with optimal initial transmission ensuring), and leads to a rising of the energy within the limits of 15%.

2.2 Optimization of the pumping beam cross-section

As follows from (3), as well as from general reasoning, the energy increases when the initial inversion, n_{ai} , increases. The law describing an inversion increase during the time interval between laser pulses may be defined from the

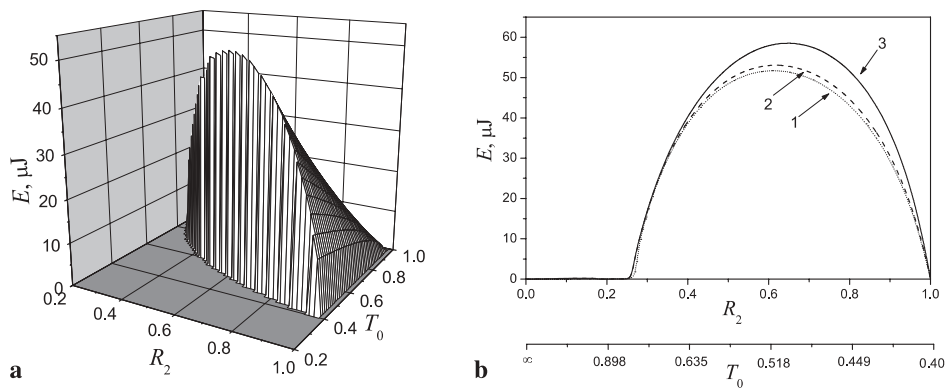


FIGURE 1 The laser pulse energy dependencies from: **a** the output mirror reflectivity R_2 and the initial transmission T_0 ; **b** the output mirror reflectivity R_2 if the initial transmission is calculated by (7) (plot 1 for $n_{s0} = 10^{17}$ cm^{-3} , plot 2 for $n_{s0} = 10^{18}$ cm^{-3} , plot 3 for $n_{s0} = 10^{19}$ cm^{-3})

first system equation (1) at $q = 0$. After the integration one obtains:

$$n_a = n_{a\max} - (n_{a\max} - n_{af}) \exp\left(-\frac{t}{\tau_{fa}}\right), \quad (8)$$

where time is counted from the previous pulse ending.

The interval between the laser pulses Δt and their frequency F may be easily determined from (8) if it is taken into account that the pulse duration for such lasers has $t_p \ll \Delta t$, and the inversion before the laser pulse is $n_a = n_{ai}$, to yield:

$$\Delta t = \frac{1}{F} = \tau_{fa} \ln\left(\frac{n_{a\max} - n_{af}}{n_{a\max} - n_{ai}}\right). \quad (9)$$

As mentioned above, the maximal achievable value of the inversion is defined by the pumping and the generating medium parameters, and amounts to $n_{a\max} = \frac{\eta P_p}{V h \nu_p} \tau_{fa}$. On the other hand, this value can obviously not exceed the active ion concentration in the generating medium, n_{a0} , (as it is known that the concentration quenching of the luminescence restricts the value of the activator ion concentration, n_{a0} , on the nearby level of 1 at. % for Nd:YAG). This condition allows the determination of the value of the pumping power density, thus ensuring the maximum possible inversion level achievement:

$$\frac{\eta P_p}{\pi r_p^2 l_a} = \frac{n_{a0} h \nu_p}{\tau_{fa}}. \quad (10)$$

If the pumping power ηP_p and the generating medium length l_a are fixed, the pumping power density can only be changed by means of the pumping beam radius r_p . A pumping beam radius decrease at fixed ηP_p and l_a , leads to a pumping power density rise, as well as a rise of the inversion upto a value of $\sim n_{a0}$, and so leads to an energy increase. However, at low enough values of r_p , the energy begins to decrease because of a generation volume decrease (see (3)). Hence an optimal value of the pumping beam radius $r_{p\text{opt}}$ must exist. The estimation of $r_{p\text{opt}}$, may be obtained from the $E = E(r_p)$ dependence calculation for the different effective pumping power values, at which every computed point of the optimization of the initial transmission and the output mirror reflectivity, will be realized as stated above. The results of these calculations are presented in Fig. 2a,b.

The specific peculiarity of the curves on Fig. 2a is the presence of a sharp asymmetrical “threshold-like” extremum near $r_p = r_{p\text{opt}}$. The inversion in the extremum for all the curves amounts to n_{a0} , as it follows from the comparison of

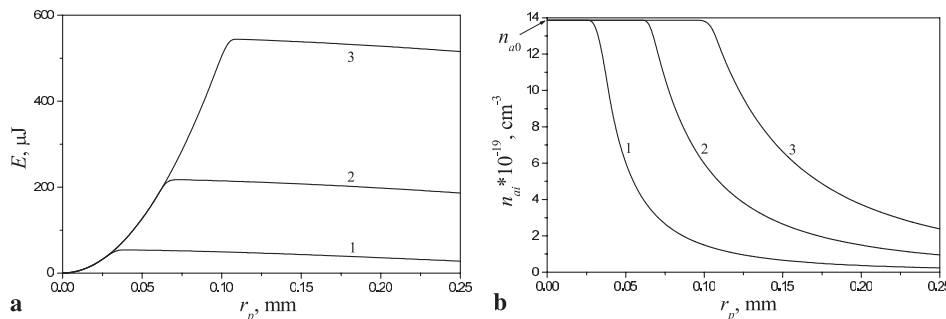


FIGURE 2 The dependencies of the laser pulse energy (a) and the initial inversion (b) from the pumping beam radius for the different values of the effective pumping power: $\eta P_p = 0.5 \text{ W}$ (1), $\eta P_p = 2 \text{ W}$ (2), $\eta P_p = 5 \text{ W}$ (3)

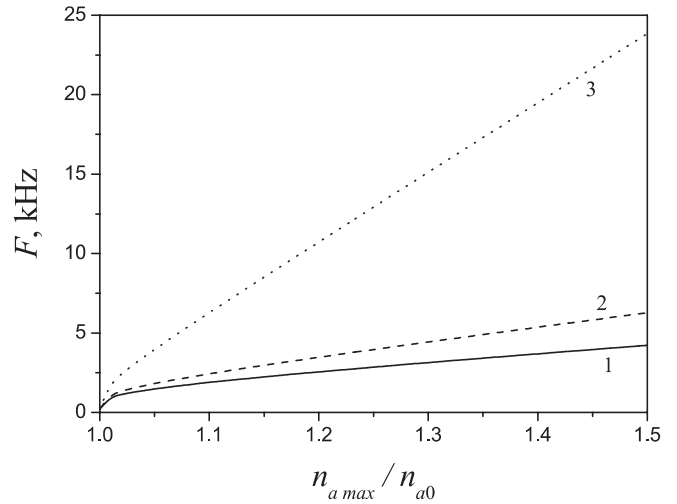


FIGURE 3 The dependency of the frequency F from the $n_{a\max}$ normalized on n_{a0} for the different values of the relation n_{af}/n_{a0} ($n_{ai} \approx n_{a0}$): $n_{af}/n_{a0} = 0.1$ (1), $n_{af}/n_{a0} = 0.5$ (2), $n_{af}/n_{a0} = 0.9$ (3)

Fig. 1a and b. More precisely, the inversion n_a remains a certain percentage less than n_{a0} , but this difference does not essentially change the value of the energy.

Thus, the optimization of the pumping beam radius may be realized by the following rule: at the fixed effective pumping power, the optical system must ensure sufficiently low values of the pumping beam radius, but not lower than the value reached at inversion, $n_{ai} = n_{a0}$, which is:

$$r_{p\text{opt}} = \sqrt{\frac{\eta P_p \tau_{fa}}{\pi l_a n_{a0} h \nu_p}}. \quad (11)$$

As Fig. 2a shows, the effective pumping power increase at $r_p = r_{p\text{opt}}$, does not lead to an energy (as well as the peak power) increase, but causes the frequency F to increase in accordance with (9). This is also obvious from energy conservation. This fact as well as the linearity of the $F(n_{a\max}/n_{a0})$ dependence at sufficiently high $n_{a\max}$ values (Fig. 3), gives the possibility of frequency control without change of the pulse parameters. This may be convenient for frequency pulse or positional pulse modulation. Note that the value $n_{a\max}/n_{a0}$ in Fig. 3 is larger than unity because $n_{a\max} = \frac{\eta P_p}{V h \nu_p} \tau_{fa}$ presents an inversion which may be theoretically achieved at a fixed value of the effective pumping power density, $\eta P_p/V$, under the assumption that any concentration limitation of $n_{a\max}$ is absent. Naturally, the inversion in the generating medium can not ex-

ceed the total active centres concentration, n_{a0} , so in fact for all points in Fig. 3, $n_{a\max} = n_{a0}$, and the abscissa axis value presents the normalized effective pumping power.

2.3 Influence of the generating medium length on laser pulse parameters

The influence of the generating medium length on the laser pulse parameters may be defined by generalization of the approach used in the previous subsection (2.2), i.e. by the determination of the initial optimal transmission and the output mirror reflectivity for the values of the r_p and l_a pairs. The calculated dependencies of the peak power and the energy from r_p and l_a for the effective pumping power 0.5 and 5 W are presented in Fig. 4.

As can be seen from Fig. 4, at high enough (≥ 1 mm) values of l_a the energy as well as the peak power is practically independent of the generating medium length, and depends only on the pumping beam radius. It should be noted that at $l_a \gg 1$ mm the single-mode generation condition $l_a \leq \frac{c0}{n\Delta\nu_a}$, where $\Delta\nu_a$ is the amplification outline width, will be not satisfied. This inessential dependence of energy upon the generating medium length allows use of either bulk single crystals or epitaxial film gain medium.

Thus, the achievement of the microchip Q-switched laser optimization for the maximal energy in the laser pulse, while taking into account the analysis of sections 2.1–2.3, amounts to the following: at a given effective pumping power value,

and a constructively chosen (with wide enough limits) generating medium length, the optimal pumping beam radius is determined from (11). After that, the optimal values of the initial transmission and the output mirror reflectivity are defined by the $E = E(R_2)$ dependence calculation, taking into account the relationship between R_2 and T_0 (7). At the defined value of the initial transmission, the highest energy value is realized if the phototropic centers concentration in the absorber is set at the maximum reachable with current technology. In this way the optimization of the microchip Q-switched laser parameters is in fact reduced to a one-parametric case of either, the output mirror reflectivity, or the absorber initial transmission.

3 A comparative analysis of Q-switched microchip lasers based on Nd : YAG and Yb : YAG generating media

Here we use the previously mentioned approach for comparison of the Q-switched Yb : YAG laser characteristics with those of the more traditional Nd : YAG laser. As mentioned in the introduction, the features of the Yb : YAG medium allow expectation of the achievement of higher energy values with it, in comparison with Nd : YAG. The calculations are based on the absorbed pumping power, not on the effective pumping power ηP_p , because of the sufficient difference in the Stox losses for Yb : YAG and Nd : YAG. The generating medium length l_a , amounts to 1 mm, and the

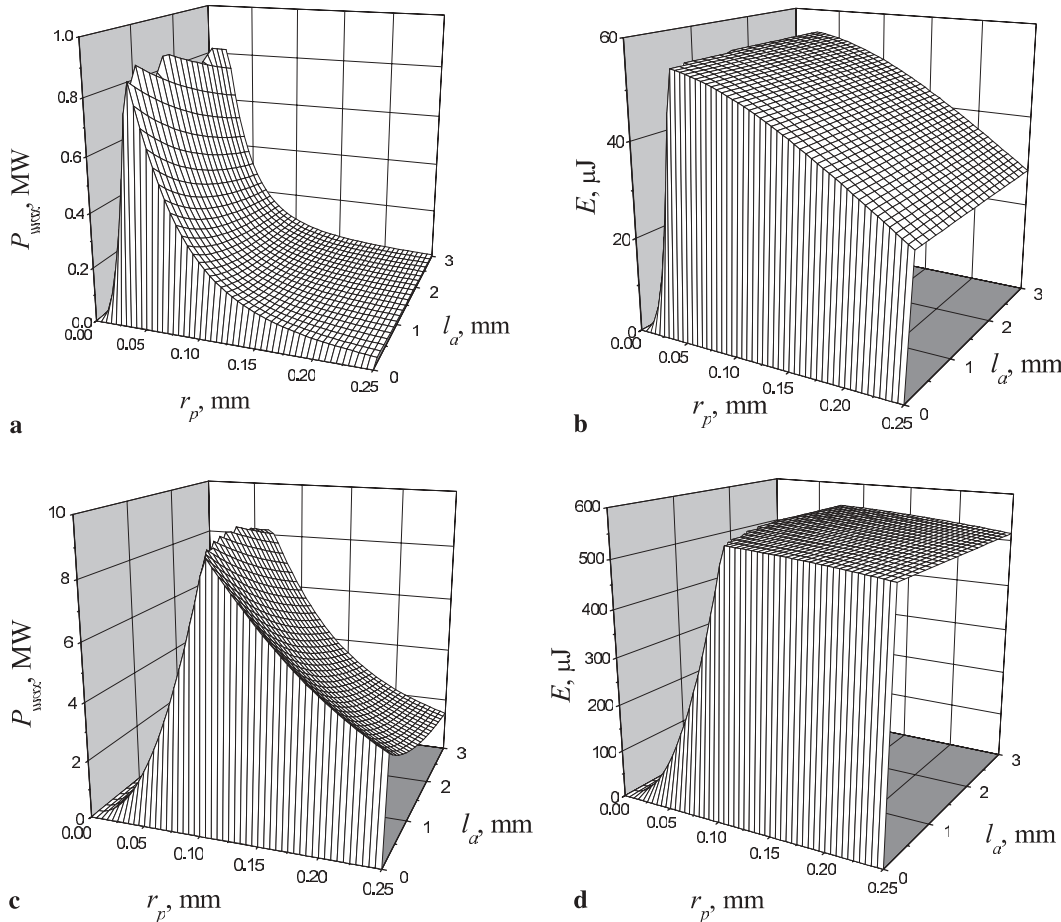


FIGURE 4 The dependencies of the peak power (a, c) and the energy (b, d) from the pumping beam radius r_p and the generating medium length l_a at the values of the effective pumping power 0.5 W (a, b) and 5 W (c, d)

Yb^{3+} concentration $n_{a0} = 26.6 \times 10^{20} \text{ cm}^{-3}$ [5]. The diffraction losses and losses into the material L_i for both media are considered to be equal, with $L_i = 0.03$.

The optimization is now realized by the following process: for each value of the absorbed pumping power P_a , the optimal value of the pumping beam radius is calculated from (11). Then the optimal value of the output mirror reflectivity R_2 , and the absorber initial transmission T_0 , related to R_2 as per (7), are determined by the $E(R_2)$ dependence computation. Such a calculation allows the estimation of the highest theoretically reachable values of the peak power and the energy in the laser pulse at the given absorbed pumping power P_a value.

As follows from our calculations, the optimal pumping beam radii $r_{p\text{opt}}$ for Nd:YAG and Yb:YAG, are defined by expressions $r_{p\text{opt}} = 40 \sqrt{P_a} \mu\text{m W}^{-1/2}$, and $r_{p\text{opt}} = 22 \sqrt{P_a} \mu\text{m W}^{-1/2}$, respectively, i.e. the optimal radius for Yb:YAG is almost in twice as low. This complicates the optimal pumping beam radius achievement for the Yb:YAG laser at low values of the absorbed pumping power (particularly at the low values of P_a , as diffraction restrictions become essential).

The results for the peak power and energy as a function of the absorbed pumping power calculations are shown in Fig. 5.

As shown in Fig. 5, the substitution of the Nd:YAG generating medium with that of the Yb:YAG under the condition $r_p = r_{p\text{opt}}$, leads essentially to the increasing of the energy as well as the peak power of the laser pulse. The linearity of the $P_{\text{max}} = P_{\text{max}}(P_a)$ and $E = E(P_a)$ dependencies, allows estimation of the highest possible values of the energy and the peak power for the different pumping power values. In particular, for the absorbed pumping power value $\sim 5 \text{ W}$, the maximal values of the energy is 0.4 mJ for Nd:YAG and 3 mJ

for Yb:YAG laser, at the peak power nearby 7 and 86 MW respectively.

As follows from our calculations, if the condition $r_p = r_{p\text{opt}}$ is fulfilled, the maximum reachable values of the peak power and the energy are realized at the output mirror reflectivity R_2 and are the same for all values of the absorbed power, which follows directly from the expressions (2)–(4). At $n_{ai} = n_{a\text{max}}$ and with the relationship (7) satisfied, the final inversion n_{af} is determined only by R_2 , so the peak power and energy are also determined by the output mirror reflectivity only. The significance of the optimal pumping beam radius $r_{p\text{opt}}$, and the pumping power P_p is to ensure achievement of the maximum initial inversion value $n_{a\text{max}}$. It must be mentioned, that the obtained value of the optimal output mirror reflectivity amounts to ~ 0.1 (Fig. 6). If the pumping beam radius increases from $r_{p\text{opt}}$, the optimal reflectivity also increases and at high enough $r_p \sim 250 \mu\text{m}$ it amounts to ~ 0.95 , which corresponds to the output mirror reflectivity, generally accepted for the lasers. As can be seen in Fig. 6, increasing the output mirror reflectivity from its optimal value leads to a decrease in the energy required for a sufficiently high absorbed pumping power.

The energy and the peak power maximums for the Yb:YAG medium conforms to the lower values of the output mirror reflectivity in comparison with the Nd:YAG laser. In particular, the peak power maximums for Yb:YAG and Nd:YAG are realized at $R_2 \approx 0.02$ and 0.09 respectively (if $r_p = r_{p\text{opt}}$), with energy maximums – at $R_2 \approx 0.04$ and 0.08. This assertion is valid for an arbitrary pumping beam radius. Such a peculiarity comes about as a result of the relatively low value of amplification, $\sigma_a \cdot n_a$, for the Yb:YAG crystal.

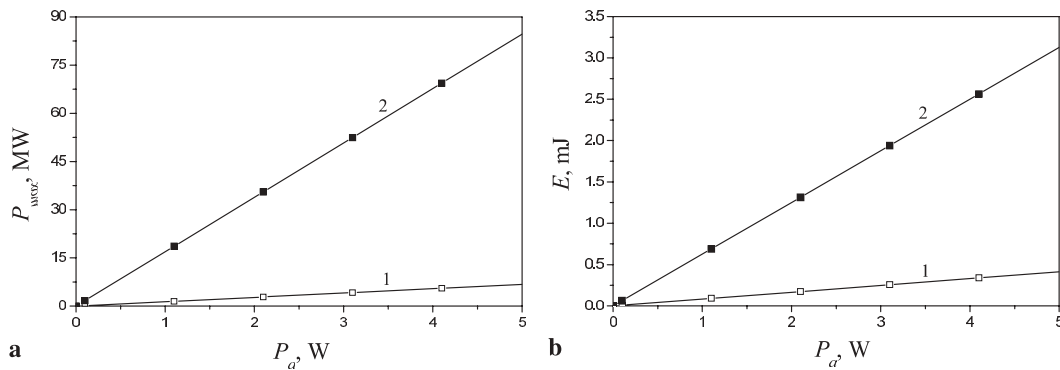


FIGURE 5 The highest reachable peak power (a) and energy (b) in the laser pulse as a function from the absorbed pumping power for Nd:YAG (1) and Yb:YAG (2) Q-switched lasers

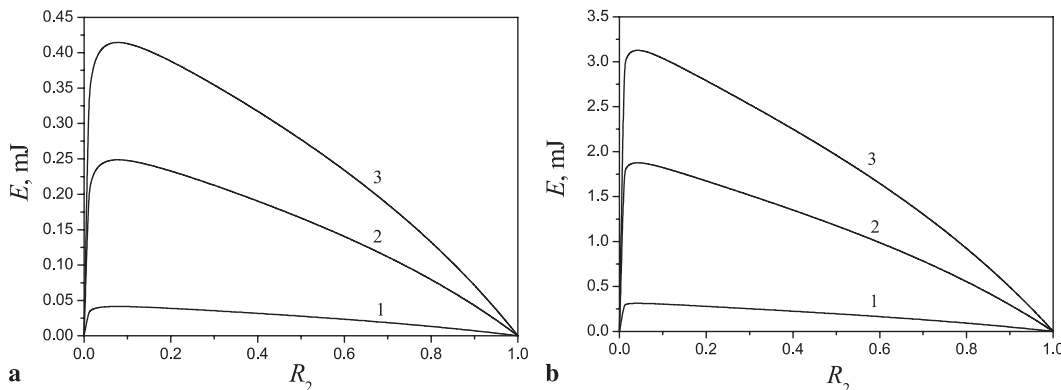


FIGURE 6 The dependencies of the Nd:YAG (a) and Yb:YAG (b) lasers energy from the output mirror reflectivity for the different values of the absorbed pumping power: $P_a = 0.5 \text{ W}$ (1), $P_a = 3 \text{ W}$ (2), $P_a = 5 \text{ W}$ (3)

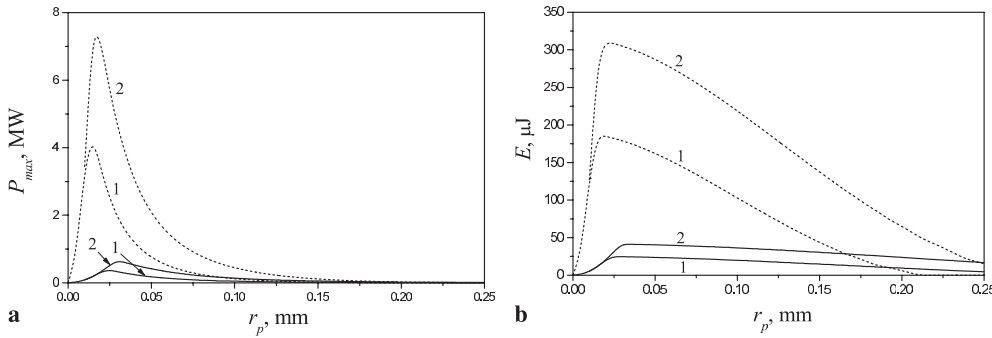


FIGURE 7 The peak power (a) and the energy (b) dependencies from the pumping beam radius for Nd:YAG (solid line) and Yb:YAG (dash line) lasers at the absorbed pumping power $P_a = 0.3$ W (1) and $P_a = 0.5$ W (2)

If the pumping beam radius increases from $r_{p, \text{opt}}$ at a fixed pumping power, this may lead to sufficient changing in the Nd:YAG and Yb:YAG generating media efficiencies relationship. In Fig. 7 the peak power and the energy dependencies from the pumping beam radii are shown for Nd:YAG and Yb:YAG lasers at the values of the absorbed pumping power $P_a = 0.3$ and 0.5 W. As shown in Fig. 7, at low values of the pumping power, and high enough r_p , the energy as well as the pumping power of the Nd:YAG laser becomes higher than that of the Yb:YAG laser. Thus, the efficiency of the Yb:YAG generating medium will certainly become apparent at a sufficiently high pumping power.

4 Conclusions

The conclusions of our work can be summarised as follows:

- 1) Maximal energy in the microchip Q-switched laser pulse is achieved if the laser action takes place just above the generation threshold. The generation condition (6) allows establishment of the connection between the optimal values of the initial transmission and the output mirror reflectivity (7).
- 2) At the fixed values of the initial transmission and the output mirror reflectivity, the energy increases if the tetravalent chromium ion Cr^{4+} concentration increases (at respectively lower absorber thicknesses). Relative rising of the energy is about 13%, if Cr^{4+} concentration increases from 10^{17} to 10^{19} cm^{-3} . This value also corresponds to the measure of inaccuracy of the rough analytical expressions (2), (3).
- 3) The energy and the peak power essentially depend on the pumping beam radius especially if the pumping power is low. The maximal values of the energy, as well as the peak power, are achieved at some optimal pumping beam radius, determined by the effective pumping power, the generating medium length, and the maximal reachable inversion value.
- 4) The effective pumping power increase at $r_p = r_{p, \text{opt}}$ does not lead to the energy (as well as the peak power) increasing, but causes a frequency increase in accordance with (9). This gives the possibility of frequency control without changing the pulse parameters, which may be convenient

for pulse frequency modulation or positional pulse modulation.

- 5) At sufficiently high (≥ 1 mm) generating medium length l_a , the value of the energy in the pulse does not essentially depend on the generating medium length. Such inessential dependence allows it to be used for either bulk single crystals or epitaxial films.
- 6) The substitution of the Nd:YAG generating medium with the Yb:YAG laser under the condition $r_p = r_{p, \text{opt}}$ leads to an increase of energy as well as peak power in the laser pulse.
- 7) Increasing the pumping beam radius from $r_{p, \text{opt}}$ at the fixed pumping power leads to sufficient change in the Nd:YAG and Yb:YAG laser efficiencies relationship. In particular, at low values of pumping power and a high enough pumping beam radius, ($\sim 200 \mu\text{m}$), the energy and peak power in the pulse of the Nd:YAG laser becomes greater than that of the Yb:YAG. Thus, the efficiency of the Yb:YAG generating medium becomes apparent at sufficiently high values of pumping power.
- 8) The value of the optimal pumping beam radius for the Yb:YAG generating medium is approximately twice as low as the optimal radius for the Nd:YAG medium. This complicates the optimal radius achievement for the Yb:YAG laser. Moreover, the Yb:YAG laser is more sensitive to changes in the pumping beam radius, so it may require a more precise focusing system.

REFERENCES

- 1 T. Dascalu, G. Philipps, H. Weber: *Opt. Laser Technol.* **29**(3), 145 (1997)
- 2 F.D. Patel, E.C. Honea, J. Speth, S.A. Payne, R. Hutcheson, R. Equall: *IEEE J. Quant. Elec.* **QE-37**(1), 135 (2001)
- 3 V. Müller, V. Peters, E. Heumann, M. Henke, K. Petermann, G. Huber: *OSA Trends in Optics and Photonics, Advances in Solid State Lasers*, Tech. Digest, 68 (2002) p. MD4
- 4 Z. Merzyk: *Non-linear absorbers*. Warszawa, Wojskowa Akademia Techniczna 2000, in Polish
- 5 J. Dong, P. Deng, Y. Liu, Y. Zhang, J. Xu, W. Chen, X. Xie: *Appl. Opt.* **40**(24), 4303 (2001)
- 6 G.M. Zverev, J.D. Golijajev, E.A. Shalaev, A.A. Shokin: *Lasers on the aluminium yttrium garnet with neodymium*. Moscow, Radio i svias 1985, in Russian
- 7 I.M. Syvortoka, S.B. Ubizskii, S.S. Melnyk, A.O. Matkowski, K. Kopyński, Z. Mierczyk: Growth and optical absorption of $\text{GGG}:\text{Mg}^{2+}\text{Cr}^{4+}$ epitaxial films. Conf. on Lasers, Electro-optics (CLEO EUR. 2000). Sept. 10–15, Nice, France, Conf. Digest, p. CWF-29